Curvature motion for union of balls

THOMAS LEWINER[1,2], CYNTHIA O.L. FERREIRA[1], MARCOS CRAIZER[1] AND RALPH TEIXEIRA[3]

[1] Department of Mathematics — Pontifícia Universidade Católica — Rio de Janeiro — Brazil
[2] Géométrica Project — INRIA – Sophia Antipolis — France
[3] Fundação Getulio Vargas — Rio de Janeiro — Brazil
{tomlew, cynthia, craizer}@mat.puc--rio.br. ralph@fgv.br.

Abstract. This work proposes a scheme for multi–resolution representation of union of balls in the plane. This representation is inspired by curvature motion for smooth curves. More precisely, the proposed evolution of centres and radii of the balls are based on equations of evolution of the medial axis of a curve that performs curvature motion. The results obtained are very close to the pixel approximation of curvature motion.
Keywords: ***Union of Balls. Medial Axis. Curvature Motion. Shape. Vision. Multiresolution.***

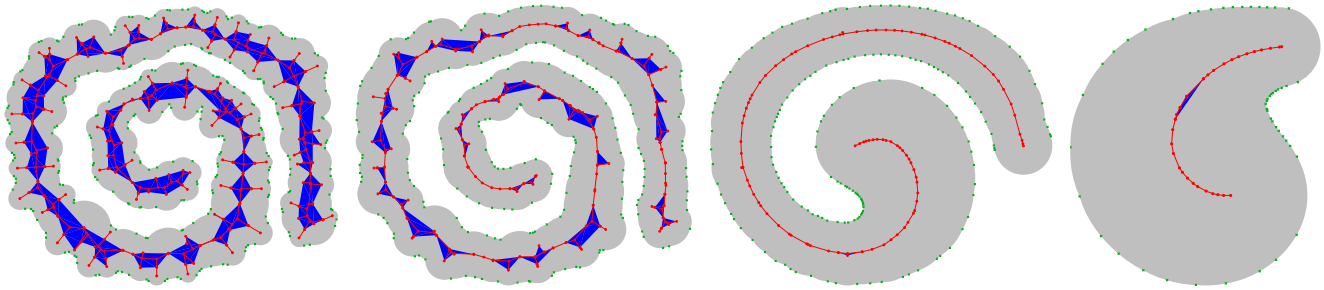

Figure 1: *Curvature motion on a spiral shape made of a union of balls.*

1 Introduction

In this paper we shall consider finite union of balls in the plane. The objective is to describe a motion that represents the union of balls in multi–resolution, i.e., such that at each time the new union of balls can be considered a rough version of its predecessor. In other words, we are constructing a scale space for unions of balls.

Importance of curvature motion. Curvature motion is a method for simplifying smooth curves that has very desirable properties: A curve does not create self–intersections, two different curves do not intersect, any curve become convex in finite time and at the end the region become close to a disk. Thanks of these properties, curvature motion is widely used for creating multi–resolution representation of plane regions [12, 10, 11]). Some generalizations of curvature motion to surfaces in 3D-space are also widely used for simplifying surfaces [9, 6].

Union of balls as discretization of shapes. Pixel discretization of curvature motion is a delicate task [3]. Instead, we can consider a region $\mathcal{U}$ in the plane and its medial axis, which consists in the centres of maximal balls contained in the region. In this way, the region $\mathcal{U}$ can be written as an infinite union of balls whose centres lie in the medial axis. By sampling these centres, one can approximate $\mathcal{U}$ by a finite union of balls [1]. Our main point of view is to consider union of balls as a discretization of the region $\mathcal{U}$, but we are also pointing at objects that are modelled as union of balls, such as molecules.

Contributions. In this article, we propose a multi–resolution representation of union of balls that is inspired by curvature motion. The equations of evolution of centres and radii of the balls are based on the equations of evolution of the medial axis and the radius function of a smooth curve evolving by curvature motion [13, 14]. The main expectation is that, if the balls sampling at the medial axis is dense enough, the proposed movement will be close to the curvature motion.

There are several difficulties in the implementation of the motion, which are explained and solved in this paper. Since it is based on the medial axis of a union of balls, we need to have reliable implementations of Voronoi diagrams and α–shapes. But the points considered are often in the same circle, which makes the usual implementations quite unstable. Another difficulty is the bad sampling of the balls in the medial axis. Even if one begins with evenly spaced

Preprint MAT. 15/05, communicated on May 15^{th}, 2005 to the Department of Mathematics, Pontifícia Universidade Católica — Rio de Janeiro, Brazil. The corresponding work was published in the proceedings of the Sibgrapi 2005, pp. 47–54. IEEE Press, 2005.

balls, several times the new centres become too close or too far from each other. When this occurs, it is necessary to over–sample or to sub–sample the balls. And last but not least, there are a lot of numerical problems in the curvature and radius derivatives estimations.

Overview. This paper is organized as follows: In section 2 *Medial axis of a union of balls* we describe the theoretical background related to medial axes and α–shapes necessary to understand the paper. Then, section 3 *Curvature motion on the medial axis* recalls and completes the results of [13] for the effects of curvature motion on the medial axis. In section 4 *Proposed evolution for union of balls* we describe the proposed equations for the centres and radii of a union of balls. In section 5 *Sampling condition and numerical issues* we discuss several implementation issues and in section 6 *Results, application and conclusion* we show the results obtained. This paper is an extension of the master's dissertation of C.Ferreira [5].

2 Medial axis of a union of balls

A union of balls can be concisely described in terms of its medial axis and its α–shape. We will now summarize these two notions, which were first described in [4] and [2].

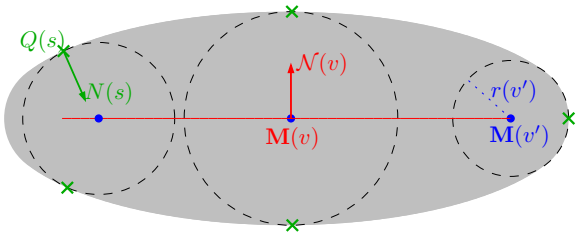

Figure 2: *Medial axis of an ellipse.*

Medial axis of a region. The (inner) medial axis of a region is the set of points of the region whose distance to the boundary is reached in at least two points (Figure 2). This notion is close to the (inner) skeleton of a region, which is the closure of the medial axis. The distance from a point of the medial axis to the boundary of the region is called the radius function.

Generically, the medial axis of a smooth region is a finite graph whose edges are smooth curves [13]. If the region is the interior of a polygon, the medial axis is the boundary of the cells of its Voronoi diagram. An extension of this property will allow a direct construction of the medial axis of a union of balls from the Voronoi Diagram of the intersection points of the boundary of the balls.

α–shape. The α–shape of a union of balls in the plane is a combinatorial structure made of triangles, edges and vertices. Intuitively, it describes if neighbouring balls intersect, constructing an edge or a triangle to materialize this intersection. By varying the α, one can interpret if the balls intersect deeply or simply touch. In the remaining of the paper, we will consider only the case $\alpha = 0$. Here follows a brief definition of the α–shape which will be used mainly for the implementation issues of section 5 *Sampling condition and numerical issues*.

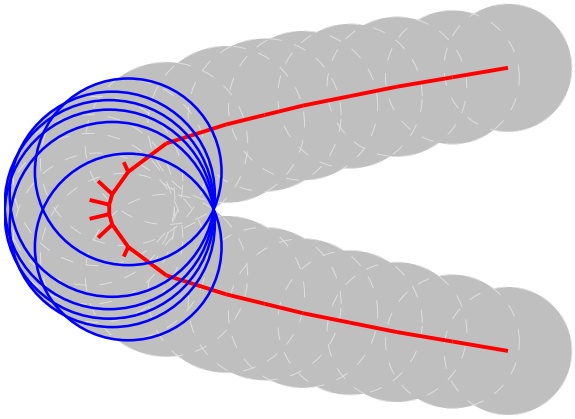

Figure 3: *Generally, the Voronoi balls (thick) are not part of the original union (dotted).*

The α–shape of a set of points $\mathcal{U} = \{\mathbf{p}_i\}$ is defined as follows: The vertices of the α–shape are the points $\mathbf{p}_i$. A triangle $\mathbf{p}_i\mathbf{p}_j\mathbf{p}_k$ belongs to the Delaunay triangulation if its circumcircle does not contain any point of $\mathcal{U}$ except $\mathbf{p}_i$, $\mathbf{p}_j$ and $\mathbf{p}_k$. It further belongs to the α–shape if its circumradius is inferior to α. An edge $\mathbf{p}_i\mathbf{p}_j$ of a Delaunay triangle belongs to the α–shape if it is in the boundary of a triangle of the α–shape or if its diameter is inferior to 2α and if the distance of its midpoint to $\mathbf{p}_k$ and $\mathbf{p}_l$ is greater than α, where $\mathbf{p}_i\mathbf{p}_j\mathbf{p}_k$ and $\mathbf{p}_i\mathbf{p}_j\mathbf{p}_l$ are the two Delaunay triangles $\mathbf{p}_i\mathbf{p}_j$ bounds.

Consider now a union of balls $\mathcal{U} = \cup B_i$ and assume that $\mathcal{U}$ cannot be written as the union of a proper subset of the balls B_i. The power of a point $\mathbf{p}$ to a ball B_i of centre $\mathbf{c}_i$ and radius r_i is defined by $\pi(\mathbf{p}, B_i) = d(\mathbf{p}, \mathbf{c}_i)^2 - r_i^2$. The α–shape (Figure 5)of $\mathcal{U}$ is constructed similarly to the α–shape of a set of points, replacing the Euclidean distance for defining the circumcircle and the diametrical circle by the power distance and allowing the circumradius to be negative when the 3 balls intersect.

Medial axis of a union of balls. The medial axis is contained in the α–shape. Actually, when the α–shape has locally no triangle, the medial axis is the α–shape and the centres of balls of this part of the α–shape are the vertices of the medial axis [2].

Inside a group of triangles, the construction of the medial axis is not so straightforward, and requires the construction of the intersection points n_j of balls that lie on the boundary of the region: $n_i \in \partial\mathcal{U}$ (Figure 4). The α–shape actually fastens the computation of these intersection points.

Inside a group of triangles of the α–shape, the medial axis coincides with the edges of the Voronoi diagram of the intersection points $\{n_i\}$ [2]. The vertices $\mathbf{c}$ of this part of the medial axis are associated with the radius r of their Voronoi region, and the pairs $(\mathbf{c}, r)$ define balls that will be called

The corresponding work was published in the proceedings of the Sibgrapi 2005, pp. 47–54. IEEE Press, 2005.

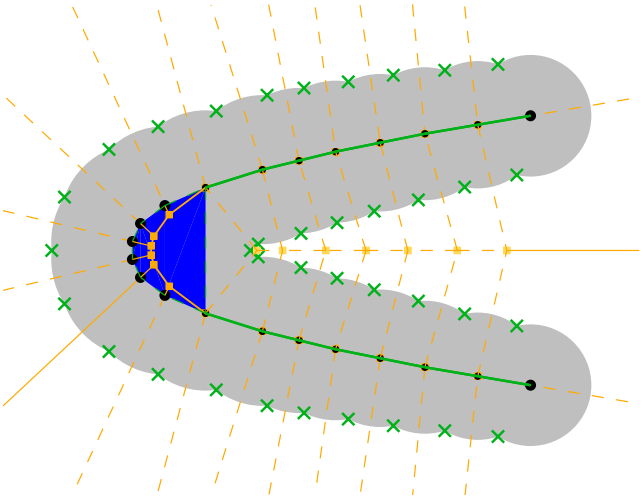

Figure 4: *The medial axis as part of the α–shape edges (solid lines) and part of the Voronoi diagram (dashed lines) of the external intersection points (cross marks).*

the *Voronoi balls* of the medial axis. Note that those Voronoi balls do not usually coincide with any ball of $\mathcal{U}$ (Figure 3).

3 Curvature motion on the medial axis

In this section we will introduce briefly the curvature motion that we intend to mimic. We will refer intensively to the geometrical description of the effects of curvature motion on the medial axis of [13] for the regular case, and to the topological evolution of [14] for the singular case (Figure 1 and Figure 6). We summarize these results here, and complete them by a geometric description of the evolution of the end points.

Curvature motion. Consider an evolution $Q(s,t)$ of an initial simple curve $Q(s,0)$ in the plane. The curvature motion [12] will deform the curve according to the equation

$$Q_t(s,t) = K(s,t)N(s,t)$$

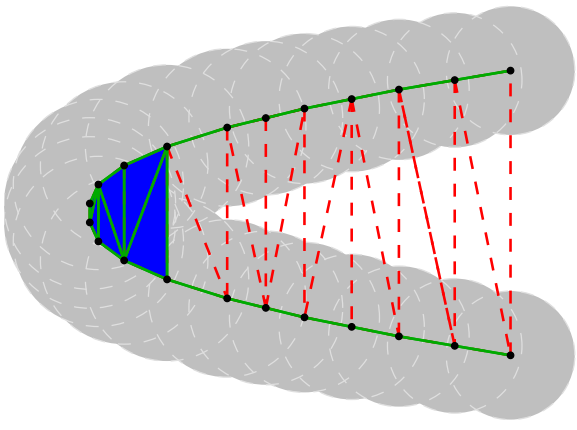

Figure 5: *The α–shape (solid lines and filled triangles) as a subset of the regular triangulation (dashed lines).*

where $K(s,t)$ is the curvature and $N(s,t)$ is the inward unit normal (Figure 2).

In the rest of this work, we will consider that the medial axis $\mathbf{M}(v)$ is parameterized by the arc–length (near the regular points) and denote by $\mathcal{K}$ its curvature and $\mathcal{N}$ its unitary normal. The radius at point $\mathbf{M}$ and its derivatives are denoted by r, r_v and r_{vv}.

Curvature motion around a regular point. A point $\mathbf{M}$ of the medial axis is called *regular* if the maximum ball centred at $\mathbf{M}$ is tangent to the boundary at exactly 2 points, with a tangency of order 1. It was shown in [13] that when the curve evolves by curvature motion, a regular point evolve according to equations

$$\begin{cases} \mathbf{M}_t = \frac{\mathcal{K}\left(1-{r_v}^2\right)}{\left(1-{r_v}^2-rr_{vv}\right)^2-r^2\mathcal{K}^2\left(1-{r_v}^2\right)}\mathcal{N} \\ r_t = \frac{r\mathcal{K}^2\left(1-{r_v}^2\right)+r_v\left(1-{r_v}^2-rr_{vv}\right)}{\left(1-{r_v}^2-rr_{vv}\right)^2-r^2\mathcal{K}^2\left(1-{r_v}^2\right)} \end{cases} \tag{1}$$

Curvature motion at a bifurcation. When the maximal ball of a point $\mathbf{M}$ of the medial axis touches the curve at $n \geq 3$ points, we call $\mathbf{M}$ a bifurcation point. Generically, a bifurcation point is the intersection of n curves called symmetry sets for which it is a regular point [14]. Hence the evolution of a bifurcation point can be seen as the evolution of the intersection of n symmetry sets evolving according to equation (1).

Curvature motion at an end point. When the maximal disk of a point $\mathbf{M}$ of the medial axis (actually the skeleton) touches the curve at only one point $\mathbf{p}$, the order of tangency must be at least 3 [14]. We call such a point $\mathbf{M}$ an *end point*. When the curve evolves through the curvature motion, end points of the medial axis evolve according to the following formula:

$$\begin{cases} \mathbf{M}_t = -K_{ss}\mathbf{N} \\ r_t = -K_{ss} - K \end{cases} \tag{2}$$

where K is the curvature at $\mathbf{p}$ and N is the inward normal. This formula can be proved by techniques similar to those used in [13].

4 Proposed evolution for union of balls

This works aims at constructing a curvature motion for a union of balls. Our paradigm considers that the balls forming the shape are centred on the medial axis. Starting with a union of balls that does not conform to this paradigm, the equation we use together with an eventual local re–sampling of the shape will smoothly ensure the conformance of the union of balls to it.

Curvature motion acts on each medial axis vertices according to the equations of the last section, depending on the type of this vertex. For each type, we describe now how to discretize the differential quantities of the equations introduced in last section.

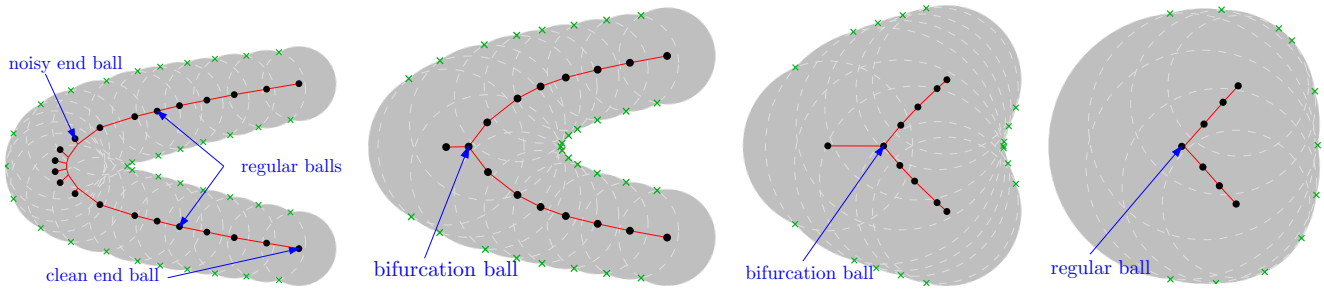

Figure 6: *The effect of the curvature motion can be computed from the medial axis.*

Inner balls. If the centre of a ball is not part of the medial axis, we shall call it an *inner ball*. Those balls are not directly necessary, but are essential since they would create a hole if removed. There is no need to have them evolved, but for numerical stability it is better to let their radius grow until they reach the boundary.

Regular balls. If the centre of a ball B belongs to the medial axis and is incident to exactly two edges of the medial axis, it is called a *regular ball* (Figure 6). These centres are alike to correspond to regular points of the medial axis, although they can correspond also to non–regular points, when the ball radius is a local maximum. In order to use equations (1) for regular points, we must estimate the curvature $\mathcal{K}$ of the medial axis and the first and second derivatives of the radius function. To do so, we will consider the maximal regular portion of the medial axis around B, i.e. a maximal sequence of adjacent regular balls containing B. This defines a polygonal line of at least 2 segments, and we can apply the method of [8] to estimate its curvature. This method can be directly adapted to estimate r_v and r_{vv}, considering r as another coordinate of each vertex of the polygonal line.

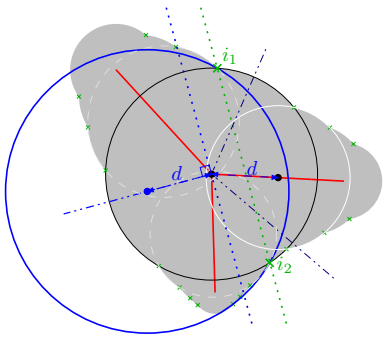

Figure 7: *At a bifurcation ball, the symmetry set continues the medial axis. Its direction is guessed as the perpendicular to the line joining the intersections i_1 and i_2. Its radius function is chosen to touch i_1 and i_2.*

Bifurcation balls. If there are more than 3 edges of the medial axis incident to its centre, the ball will be called a *bifurcation ball* (Figure 6). It is important to note that there are bifurcation points in the medial axis that are not centres of balls of the union, which we called Voronoi balls. In this case, the computation of the evolution of the bifurcation ball is not necessary, as the Voronoi balls naturally move when moving the other balls of the union.

As explained in section 3 *Curvature motion on the medial axis*, a bifurcation point should evolve as if it were a regular point of each branch of the symmetry set. The difficulty we have here is that we need points of the symmetry set that are not in the medial axis. This symmetry set corresponds to balls that touch the boundary of the shape twice, but are not completely included in the shape. The construction of such a ball is described on Figure 7.

After computing the evolution of the branches, one must find the intersection of each pair of branches. In our case, these branches are approximated by line segments. Hence each pair of segments intersects at a point and the new bifurcation point was proposed to be the barycentre of these intersections. The value of r_t was estimated as the mean of the values of r_t corresponding to each branch.

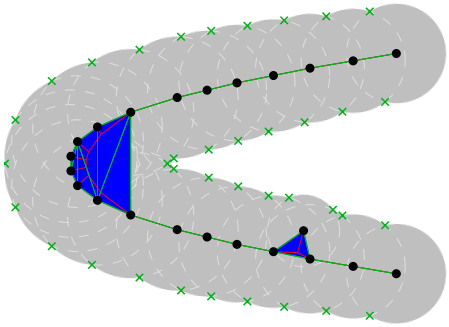

Figure 8: *A small perturbation of the shape perturbs the medial axis significantly.*

End balls. We say that a ball $B = (\mathbf{c}, r)$ is an *end ball* if there is only one edge of the medial axis incident to its centre. The medial axis is a combinatorial structure that is very sensitive to noise: a small perturbation of the boundary creates an end point close to this perturbation. The notion of perturbation is hard to formalize in general, but for the case of union of balls, we will try to make a distinction between end points that correspond to noise and end points that correspond to real protrusions: We say that an end ball is

clean if its centre is incident to only one edge of the α–shape, and *noisy* if its centre is incident to at least one triangle of the α–shape (Figure 8). The notion of "real" protuberance then corresponds to a sequence of balls going towards the end point.

Ellipse approximation. In order to use equations (2) for the end point case, we must estimate the curvature K of the curve and its second derivative K_{ss} at the point $\mathbf{q}$ where the maximal ball touches the curve. To estimate K_{ss} and K at $\mathbf{q}$, we shall consider an ellipse that approximates the end ball and the adjacent ones. This ellipse is constructed with $\mathbf{q}$ being a curvature extremum. In this way, the curvature K and its second derivative K_{ss} are estimated by $K = a/b^2$ and $K_{ss} = 3(b^2 - a^2)/a^4$ where a is the half–axis passing through $\mathbf{q}$ and b is the other half–axis.

Clean end balls. For the case of clean end balls, there is only one ball $B' = (\mathbf{c}', r')$ adjacent to B in the α–shape. We can consider that the approximating ellipse has half–axis $b = r'$ and $a = r + d(\mathbf{c}, \mathbf{c}')$.

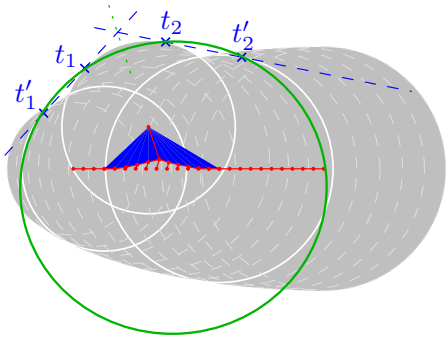

Figure 9: *For the noisy end ball case, the approximating ellipse is calculated from the bi–tangents of the end ball and the two neighbours in the boundary of the α–shape.*

Noisy end balls. For the noisy end ball case, the ellipse should follow the boundary of the union of balls. Consider the two boundary edges of the α–shape incident to the end ball B. These two edges link B to two other balls B_1 and B_2. The ellipse here will be constructed from the bi–tangent of those balls: let l_i be the external bi–tangent of B and B_i. The axis of the ellipse will be the bisector of l_1 and l_2, and the ellipse is then the unique one passing through the four tangency points t_1, t'_1, t_2 and t'_2 (Figure 9).

5 Sampling condition and numerical issues

The above description works better when the medial axis is well sampled. On one hand, as curvature motion globally shrinks the shape, the sample points will become closer during the evolution. On the other hand, when the shape is non–convex, it locally expands, making samples to get more distant. These phenomena must be compensated in order to maintain a good sampling rate.

Many difficulties appeared in the implementation of the proposed motion. Some of these difficulties are related to instability in the computation of α–shapes, Voronoi diagrams and medial axes when the points are not in general position. These cases always occur when moving slowly all the points. This section will describe the re-sampling we performed, and some solutions for numerical instabilities.

Over–sampling. The sampling is considered insufficient when two adjacent balls $B1 = (\mathbf{c}_1, r_1)$ and $B_2 = (\mathbf{c}_2, r_2)$ of the medial axis are too distant one from the other in the sense that $d(\mathbf{c}_1, \mathbf{c}_2) > \min(r_1, r_2)$. In that case, we add a new ball to the union, having centre $\frac{1}{2}(\mathbf{c}_1 + \mathbf{c}_2)$ and radius $\frac{1}{2}(r_1 + r_2)$. At each step of the evolution, this test is performed even with Voronoi balls.

Sub–sampling. The sampling will be considered too dense, leading to potential numerical errors, when two adjacent balls $B_1 = (\mathbf{c}_1, r_1)$ and $B_2 = (\mathbf{c}_2, r_2)$ of the medial axis are too close one in the sense that $d(\mathbf{c}_1, \mathbf{c}_2) < \epsilon \min(r_1, r_2)$. We chose $\epsilon = 0.05$ for the implementation. If one of the balls B_1 or B_2 is an end ball, the other one is removed. Otherwise, we substitute both balls by one with centre $\frac{1}{2}(\mathbf{c}_1 + \mathbf{c}_2)$ and radius $\frac{1}{2}(r_1 + r_2)$.

Bifurcation to regular topological change. Another test tries to remove noisy end balls, when their removal leaves the shape almost unchanged. This actually corresponds to a topological change of the smooth curvature motion described in [14], as for the transition from the third to the last step of Figure 6. The test is then performed when B_1 is an end ball, B_2 is a bifurcation ball, and $d(\mathbf{c}_1, \mathbf{c}_2) < \mu|r_1 - r_2|$. We chose $\mu = 1.05$ for the implementation.

Regular to bifurcation case. When three balls are almost intersecting, the curvature evolution can move them closer one to the others. In some cases, this topological change in inherent to the curvature motion [13], as for the transition from the first to the second step of Figure 6. In other ones, maintaining the medial axis would violate one of the conditions on the radius function described in [13]. This behaviour translates to a real numerical instability for the regular case, namely a very small denominator for equations (1). In order to estimate $\mathcal{K}$, r_v and $r_v v$ avoiding this instability, we process the same code, but replacing each ball $B_i = (\mathbf{c}_i, r_i)$ of the regular portion of the medial axis by the ball of centre $\frac{1}{2}(\mathbf{c}_i + \mathbf{c}_{i\pm1})$ and radius $\frac{1}{2}(r_i + r_{i\pm1})$. If after 10 recursions the denominator is still too small, the regular ball is considered successively as a clean end ball on one side of the medial axis, and a clean end ball on the other side. The resulting movement is computed as the average of the two clean end ball computations.

Avoiding non–existing holes. When moving the union of balls, three balls in the middle of the shape can disconnect and create an artificial hole. In order to avoid this phenomenon, a ball is added to the union of balls. This case is detected by a very small $\alpha$of a triangle T smaller than $dt \cdot r$, where dt is the time step and r is the maximal radius of the

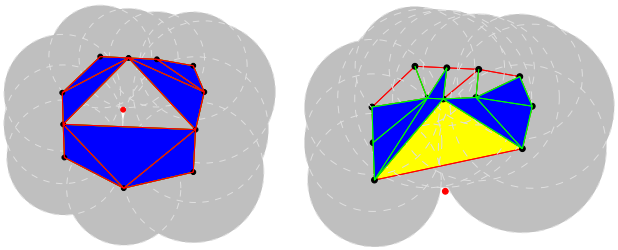

Figure 10: *Two cases where the α of triangle is small. This triangle contains a hole if it contains its radical centre (isolated point).*

balls of T. A triangle T with a small αcorresponds either to a hole in the interior of the region or to a concavity at the border of the region. To ensure that T corresponds to a hole, we check that it contain the (radical) centre $\mathbf{c}$ of its circumcircle (for the power distance) (Figure 10). In that case, we insert a ball centred at $\mathbf{c}$, with radius the minimal radius of the balls of T.

Numerical validation of the noisy end ball case. The noisy end ball case is intrinsically unstable, as it corresponds to noisy data. However, the approximation of a shape by a union of balls introduces such a noise, and that case should be handled with care. The calculus of the approximating ellipse by the bi–tangents l_i described at section 4 *Proposed evolution for union of balls* is quite stable, but the result should be validated. First, the ellipse is not well defined if the two bi–tangents are almost parallel, or if two of the four points t_1, t'_1, t_2 and t'_2 are too close. Also, the computed values of K and K_{ss} should be coherent with the original data, in particular the curvature cannot exceed the curvature of the only end ball $1/r$: $K/r > \gamma$, with γ close to 1 (we chose 0.8 for the implementation). And the curvature around the touch point $\mathbf{q}$ can be approximating by Taylor's formula: $K_i \approx K + K_s s_i + \frac{1}{2}\mathcal{K}_{ss} s_i^2$, with $K_i = 1/r_i$ is the curvature of the ball at t'_i and $s_i = d(t_i, t'_i)$. Note that around an end point, $K_s = 0$, and the validation criteria becomes: $r_i/r + \frac{1}{2} r_i K_{ss} s_i^2 > \gamma$. If one of those tests fails, the end ball is considered as clean, as the clean test is more robust.

6 Results, application and conclusion

We have implemented the proposed algorithm and the results obtained are quite promising.

(a) Comparing the proposed motion with curvature motion

In the examples considered, the proposed motion behaved qualitatively very well. In the spiral example (Figure 12), the proposed motion simplifies the curve as time evolves, without creating self-intersections, without creating holes and keeping just one connected component. These properties are very desirable for a scale space. In the "x" example (Figure 14), we have also observed that the motion simplifies the regions without creating holes and maintaining the number of connected components.

We have also compared our motion with the pixel–wise approximation of curvature motion using Megawave [9]. One can observe from (Figure 11, Figure 12, Figure 13 and Figure 14) that the behaviours of both implementations are qualitatively very close. The execution time of Megawave is related to the number of pixels of the image, while our approach depends on the number of balls describing the shape.

(b) The reaction–diffusion scale space

A multi–resolution representation of objects called reaction–diffusion scale space is proposed in [7]. In this representation, the boundary of the curve evolves according to the equation $Q_t(s,t) = (\alpha + \beta K(s,t))\, N(s,t)$ where α and β are parameters. When $\alpha = 0$, we have pure diffusion and when $\beta = 0$ we have pure reaction. By varying the ratio $\frac{\alpha}{\beta}$ we obtain descriptions of the planar shape that, in some sense, give a level of significance to parts of the shape.

We have implemented a reaction–diffusion scale space by intercalating some steps of the proposed curvature motion with some steps of erosion. The ratio between the number of steps of each motion has the same role as the ratio $\frac{\alpha}{\beta}$ of Kimia's scale space.

We can observe the results obtained on Figure 16. It is interesting to see that parts of the body are being disconnected from the main at different times, depending on the scale considered. When we apply more curvature motion, it takes more time to disconnect parts of the body, and when we apply more erosion, it takes less time for the disconnections.

We have also compared our scale space with a pixel–wise approximation of Kimia's scale space that we have implemented using Megawave. Some differences between the 2 approaches can be observed (Figure 15), but both schemes present the qualitative behaviour of a reaction–diffusion scale space.

References

[1] N. Amenta, S. Choi and R. Kolluri. The power crust, unions of balls, and the medial axis transform. *Computational Geometry: Theory and Applications*, 19(2–3):127–153, 2001.

[2] N. Amenta and R. Kolluri. The Medial Axis of Unions of Balls. *Computational Geometry: Theory and Applications*, 20(1–2):25–37, 2001.

[3] M. Craizer, S. Pesco and R. C. Teixeira. A Numerical Scheme for the Curvature Equation Near the Singularities. *J. of Mathematical Imaging and Vision*, 22(1):89–95, 2005.

[4] H. Edelsbrunner. Weighted Alpha–Shapes. Technical Report 1760, University of Illinois, 1992.

[5] C. O. L. Ferreira. Evolution of union of balls from medial axis. Master's thesis, *Math Department, PUC–Rio*, 2005.

The corresponding work was published in the proceedings of the Sibgrapi 2005, pp. 47–54. IEEE Press, 2005.

Figure 11: *Curvature motion approximated pixel–wise using Megawave: 50, 100, 150 and 200 steps.*

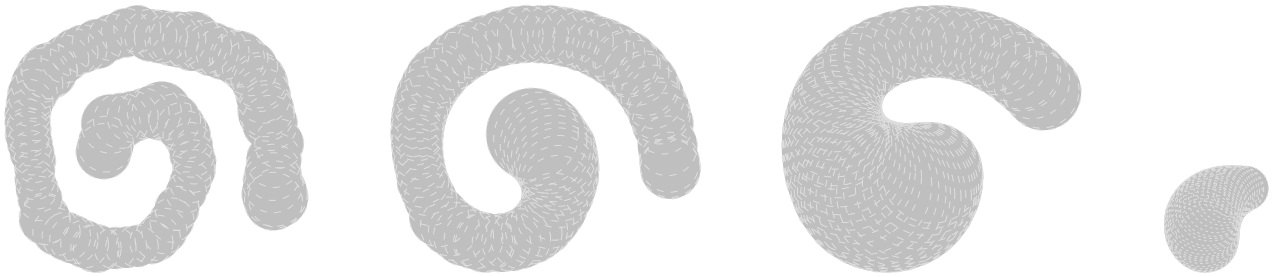

Figure 12: *Curvature motion approximated by our method: 50, 100, 150 and 200 iterations.*

[6] K. Hildebrandt and K. Polthier. Anisotropic Filtering of Non–Linear Surface Features. *Computer Graphics Forum*, 23(3), 2004.

[7] B. B. Kimia and S. W. Zucker. Shapes, Shocks and Deformations, I: The Components of Shape and the Reaction–Diffusion Space. *Computer Vision*, 15:189–224, 1995.

[8] T. Lewiner, J. Gomes Jr, H. Lopes and M. Craizer. Curvature and Torsion Estimators based on Parametric Curve Fitting. *Computers & Graphics*, 2005.

[9] F. Cao and L. Moisan. Geometric computation of curvature driven plane curve evolution. *SIAM J. of Numerical Analysis*, 3(2):624–646, 2001.

[10] F. Mokhtarian and A. K. Mackworth. A theory for multiscale, curvature based shape representation for planar curves. *Transactions on Pattern Analysis and Machine Intelligence*, 14:789–805, 1992.

[11] G. Sapiro and A. Tannenbaum. Area and Length Preserving Geometric Invariant Scale–Spaces. *Transactions on Pattern Analysis and Machine Intelligence*, 17:67–72, 1995.

[12] J. A. Sethian. *Fast Marching Methods and Level Set Methods*. Cambridge University Press, 1999.

[13] R. C. Teixeira. Medial Axes and Mean Curvature Motion I: Regular Points. *J. of Mathematical Communication and Image Representation*, 13:135–155, 2002.

[14] R. C. Teixeira. Medial Axes and Mean Curvature Motion II: Singularities. *J. of Mathematical Imaging and Vision*, 2005.

Preprint MAT. 15/05, communicated on May 15^{th}, 2005 to the Department of Mathematics, Pontifícia Universidade Católica — Rio de Janeiro, Brazil.

Figure 13: *Curvature motion approximated pixel–wise using Megawave: 50, 100, 150 and 200 steps.*

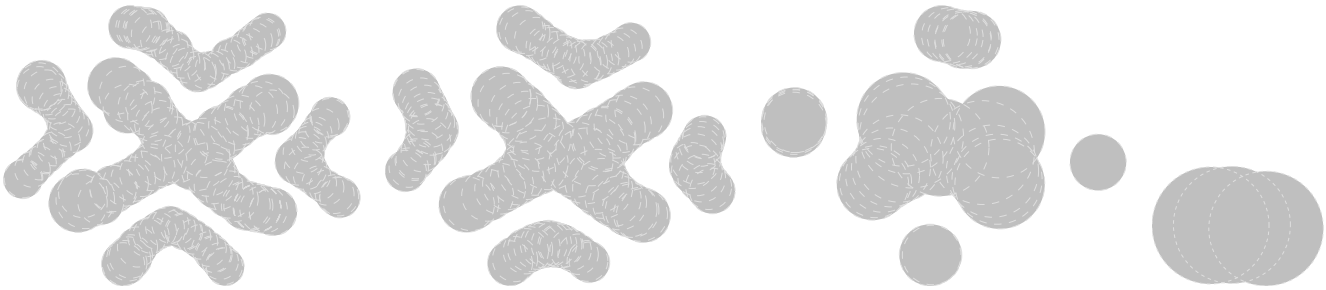

Figure 14: *Curvature motion approximated by our method: 50, 100, 150 and 200 iterations.*

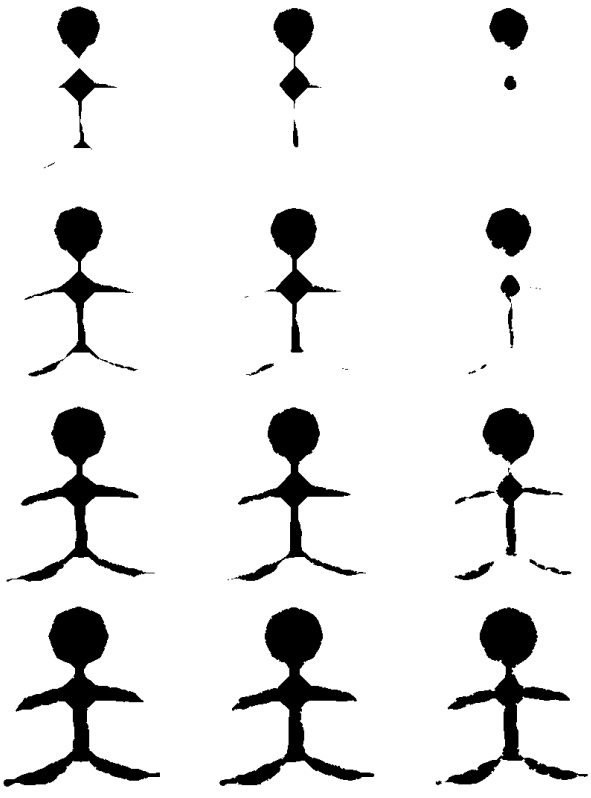

Figure 15: *Kimia scale space approximated pixel–wise using Megawave.*

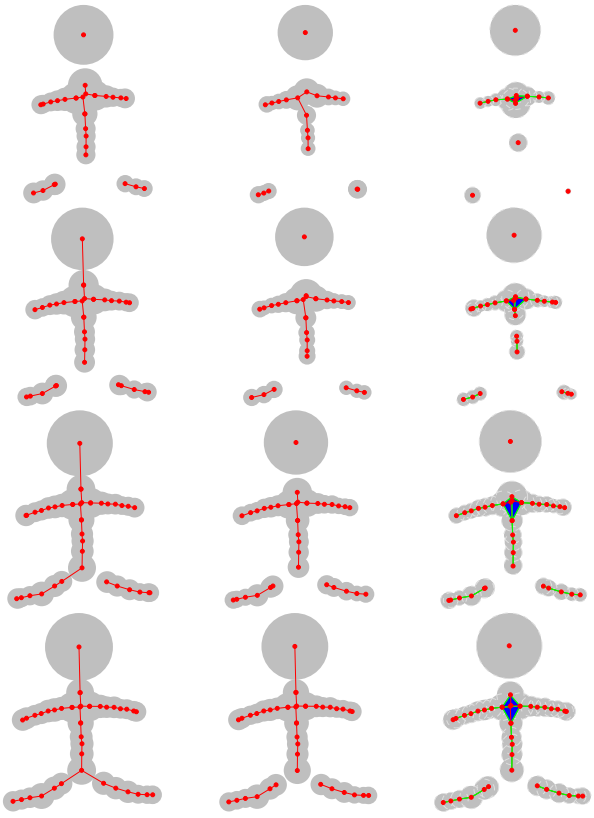

Figure 16: *Kimia scale space approximated by our method.*

The corresponding work was published in the proceedings of the Sibgrapi 2005, pp. 47–54. IEEE Press, 2005.